Rapid Identification of Soil Contamination by Pathogenic Fungi Using Single-Instance Driven Convolutional Neural Networks

Karol Struniawski[1][0000−0002−4574−2986], Ryszard Kozera[1,2,4][0000−0002−2907−8632], Aleksandra Konopka[1][0000−0003−1730−5866], Lidia Sas-Pasz[3][0000−0003−4076−4032], Agnieszka Marasek-Ciolakowska[3][0000−0001−9349−2566]

[1] Warsaw University of Life Sciences - SGGW, ul. Nowoursynowska 159, 02-776 Warsaw, Poland
karol_struniawski@sggw.edu.pl
[2] The University of Western Australia, 35 Stirling Highway, Crawley, WA 6009, Perth, Australia
[3] The National Institute of Horticultural Research, Ul. Konstytucji 3 Maja 1/3, 96-100 Skierniewice, Poland
[4] John Paul II Catholic University of Lublin, Al. Racławickie 14, 20-950 Lublin, Poland

Abstract. Microbial contamination of laboratory cultures is a major source of experimental failure and resource waste. This study proposes a Single-Instance Driven CNN approach for rapid genus-level recognition of common soil-dwelling contaminants (*Trichoderma*, *Fusarium*, *Verticillium*, *Purpureocillium*) from microscopy images. The pipeline retrieves standardized subimages and combines their predictions via majority voting to overcome the limitations of full-image classification. DenseNet201, ResNet50v2, and InceptionResNetV2 are evaluated across five datasets collected with manual, automated, and focus-stacked microscopy. The results show that subimage-based learning consistently outperforms full-image baselines, while cross-dataset experiments confirm robust generalization. Grad-CAM analysis indicates that subimage-trained networks focus on microorganism fragments and suppress irrelevant background, supporting the interpretability of the proposed workflow.

Keywords: microbial contamination, microscopy, deep learning, transfer learning, explainable AI

1 Introduction

Microbial contamination remains a critical challenge for laboratory cultures, directly affecting experimental integrity and increasing time and resource consumption [15, 11]. In routine practice, contamination is frequently detected by manual inspection of Petri dish cultures; however, this procedure is time consuming, subjective, and difficult to scale for rapid quality control [13]. The problem is

ICCS Camera Ready Version 2026
To cite this paper please use the final published version:
DOI: 10.1007/978-3-032-29909-3_14

particularly pronounced for soil-dwelling microorganisms, whose growth dynamics and morphology can lead to fast and heterogeneous contamination patterns. Several genera are especially relevant in this context, including *Fusarium*, *Purpureocillium*, *Trichoderma*, and *Verticillium* [2, 3, 5, 7, 9, 12, 14, 16, 17, 19].

Recent work has shown that machine learning can support contamination detection, yet many approaches require multiple samples, complex preprocessing, or do not generalize well across imaging protocols [8, 1]. A practical monitoring system should identify contamination reliably from a single image while remaining robust to variability in focus, illumination, and specimen preparation.

This study proposes a Single-Instance Driven CNN workflow that transforms each microscopy image into a set of standardized subimages (single instances) and combines their predictions via majority voting. We evaluate three widely used CNN backbones across five datasets acquired with different imaging protocols and demonstrate improved performance over full-image baselines. Additionally, we provide interpretability evidence through Grad-CAM analysis.

2 Materials

2.1 Dataset

Five datasets (A–E) were collected to represent common microscopy acquisition scenarios for soil-dwelling microorganisms. Datasets A and B contain manually captured images selected by expert microbiologists, while Datasets C–E were acquired using automated microscopy to reduce operator bias and increase scale. Dataset C uses wet-mount preparation with a coverslip, Dataset D uses direct smears without a coverslip, and Dataset E uses automated focus stacking to increase depth of field. Representative images are shown in Fig. 1. For the automated datasets, images with imperfect focus were retained to better reflect real laboratory conditions. Dataset sizes (instances) are: A=128 (*Verticillium* 25, *Trichoderma* 26, *Phytophthora* 20, *Fusarium* 57), B=303 (25/89/20/109 plus *Purpureocillium* 60), C=960 (*Verticillium* 240, *Trichoderma* 386, *Fusarium* 334), D=1279 (*Verticillium* 260, *Trichoderma* 240, *Fusarium* 240, *Purpureocillium* 539), and E=196 (49 per class for *Verticillium*, *Trichoderma*, *Fusarium* and *Purpureocillium*).

2.2 Single-instance retrieval

To enable learning from single instances rather than full images, we apply an image processing pipeline that extracts up to 200 candidate microorganism fragments (subimages) per input image. The pipeline follows standard machine vision procedures [6]: grayscale conversion, denoising and contrast enhancement, thresholding with morphological refinement, and connected component labeling. Components are filtered by geometric properties (e.g., area and solidity), cropped, and centered on a fixed 224×224 canvas to standardize the CNN input. The overall data flow is shown in Fig. 2.

ICCS Camera Ready Version 2026
To cite this paper please use the final published version:
DOI: 10.1007/978-3-032-29909-3_14

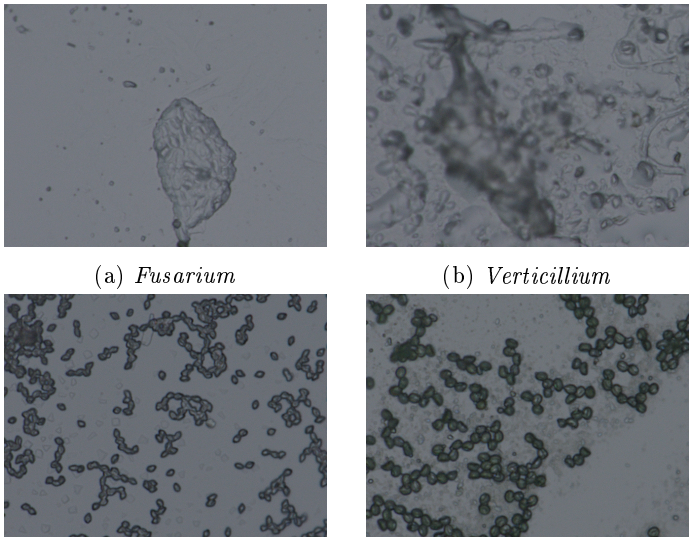

(a) *Fusarium* (b) *Verticillium*

(c) *Purpureocillium* (d) *Trichoderma*

Fig. 1: Sample images from `Dataset D`.

For each dataset, we retrieve up to 200 subimages per original image. This yields 8,432 (A), 29,432 (B), 87,991 (C), 141,951 (D), and 23,277 (E) subimages that are linked to their source images, enabling both per-subimage evaluation and image-level majority voting. Exemplary subimages are shown in Fig. 3.

3 Methodology

The retrieved subimages form the input to CNN classifiers. We employ three standard backbones (DenseNet201, ResNet50v2, and InceptionResNetV2) and apply transfer learning from ImageNet [10, 4]. Fine-tuning is performed by unfreezing selected blocks of the backbone while keeping earlier layers fixed. The classification head consists of global average pooling followed by two fully connected layers (512 neurons, Mish activation [20]) with dropout (0.3), and a softmax output.

Evaluation is reported at two levels. First, each subimage is classified independently and summarized with standard metrics. Second, for each original image, subimage predictions are aggregated using majority voting to obtain an image-level decision.

4 Results

We report performance for full images, single-instance subimages, and subimage majority voting using Precision, Recall, and AUC. We also assess robustness via cross-dataset evaluation and interpretability analysis using Grad-CAM [18].

ICCS Camera Ready Version 2026
To cite this paper please use the final published version:
DOI: 10.1007/978-3-032-29909-3_14

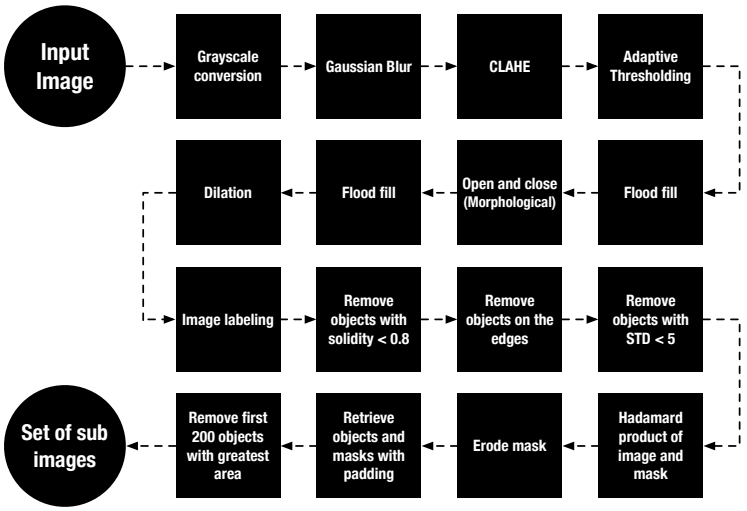

Fig. 2: The data flow diagram illustrating the proposed algorithm for subimages retrieval.

Table 1: Image-level results (Precision/Recall/AUC): subimage majority voting vs. full-image baselines.

Dataset	Method	Prec.	Rec.	AUC
C	Subimages (ResNet50v2)	0.975	0.974	0.981
C	Full image	0.405	0.399	0.581
D	Subimages (InceptionResNetV2)	0.996	0.996	0.998
D	Full image	0.609	0.607	0.753
E	Subimages (DenseNet201)	1.000	1.000	1.000

4.1 Numerical results

Across datasets and backbones, subimage-based training consistently improves performance over full-image baselines, with the largest gains observed for the automated datasets. Representative image-level Precision/Recall/AUC comparisons are summarized in Table 1.

Cross-dataset accuracy remains high across architectures, indicating that the proposed single-instance representation generalizes well between related acquisition protocols. Table 2 summarizes within-domain and cross-domain accuracy ranges.

4.2 Explainable Artificial Intelligence

To interpret model decisions, we apply Grad-CAM [18] to InceptionResNetV2 fine-tuned at different depths (block35, block17, block8) using *Fusarium* images

ICCS Camera Ready Version 2026
To cite this paper please use the final published version:
DOI: 10.1007/978-3-032-29909-3_14

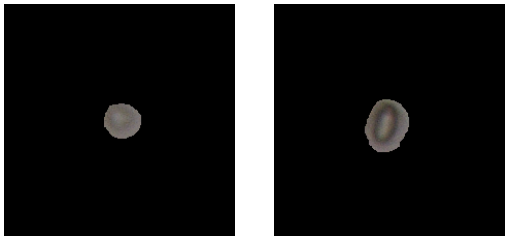

(a) *Fusarium* (b) *Verticillium*

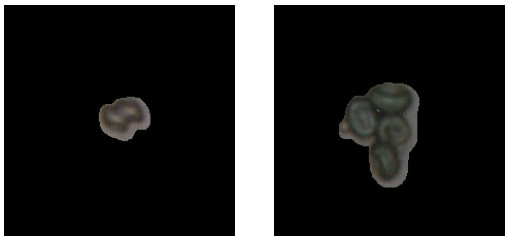

(c) *Purpureocillium* (d) *Trichoderma*

Fig. 3: Sample subimages from the retrieved `Dataset D`.

Table 2: Cross-domain accuracy ranges for image-level majority voting.

Train→Test	Accuracy
D→D	0.993–0.998
E→E	0.981–1.000
D→E	0.889–0.926
E→D	0.811–0.983

from Dataset B (Fig. 4). For full images, shallow fine-tuning can yield high scores while still highlighting background-dominant regions.

In contrast, for centered subimages the Grad-CAM maps consistently emphasize microorganism fragments and suppress the black background (Fig. 4). This supports the key assumption of the proposed workflow: single-instance standardization encourages the CNN to learn diagnostically relevant structures.

For clarity, Fig. 4 presents a compact comparison across fine-tuning depths (rows) and input types (columns).

ICCS Camera Ready Version 2026
To cite this paper please use the final published version:
DOI: 10.1007/978-3-032-29909-3_14

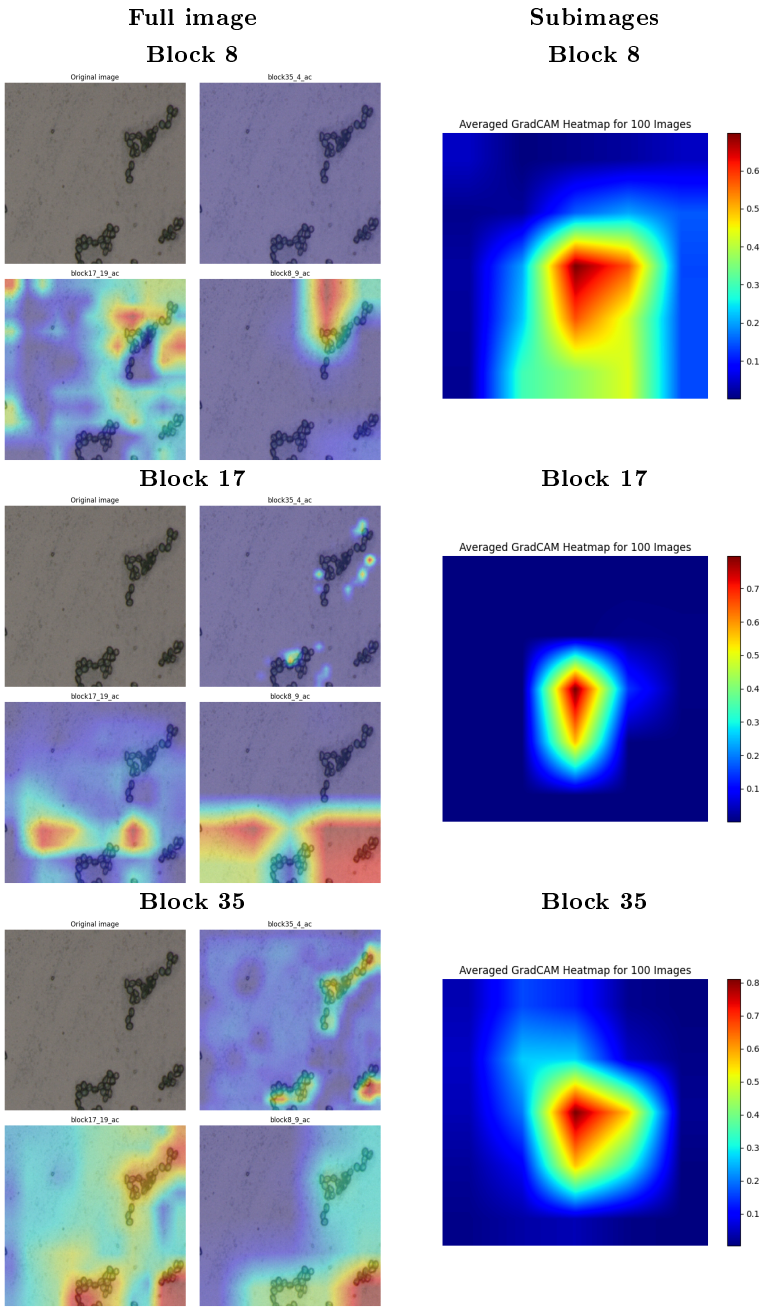

Fig. 4: Grad-CAM analysis for *Fusarium* using InceptionResNetV2 fine-tuned from different depths (rows). Left column: full image Grad-CAM. Right column: averaged Grad-CAM over random subimages. Images from Dataset B.

ICCS Camera Ready Version 2026
To cite this paper please use the final published version:
DOI: 10.1007/978-3-032-29909-3_14

5 Conclusion

This study shows that Single-Instance Driven CNNs, combined with majority voting, provide an effective and interpretable approach for identifying soil-dwelling microbial contaminants from microscopy images. Across multiple datasets and acquisition protocols, subimage-based learning improves performance relative to full-image baselines and maintains strong cross-dataset generalization. Grad-CAM analysis further indicates that single-instance standardization encourages attention to microorganism structures rather than irrelevant background. Future work may extend the approach to additional taxa and fully automated, real-time laboratory monitoring.

References

1. Amado, T.M., Bunuan, M.R., Chicote, R.F., Espenida, S.M.C., Masangcay, H.L., Ventura, C.H., Tolentino, L.K.S., Padilla, M.V.C., Madrigal, G.A.M., Enriquez, L.A.C.: Development of predictive models using machine learning algorithms for food adulterants bacteria detection. In: 2019 IEEE 11th International Conference on Humanoid, Nanotechnology, Information Technology, Communication and Control, Environment, and Management (HNICEM). IEEE (2019). https://doi.org/10.1109/hnicem48295.2019.9072907
2. Cetin, Y., Bullerman, L.: Cytotoxicity of fusarium mycotoxins to mammalian cell cultures as determined by the mtt bioassay. Food and Chemical Toxicology **43**(5), 755–764 (2005). https://doi.org/10.1016/j.fct.2005.01.016
3. Corrêa-Moreira, D., de Moraes Borba, C., Evangelista Oliveira, M.M.: Purpureocillium lilacinum: From Environment to Emergent Human Pathogens (2022)
4. Dašić, L., Pavić, O., Geroski, T., Milovanović, D., Petrović, M., Filipović, N.: Transfer learning with deep convolutional neural networks for respiratory disease classification in x-ray images. In: 2023 IEEE 23rd International Conference on Bioinformatics and Bioengineering (BIBE). pp. 176–180. IEEE (2023). https://doi.org/10.1109/bibe60311.2023.00035
5. Gastélum-Martínez, E., Compant, S., Taillandier, P., Mathieu, F.: Control of t-2 toxin in fusarium langsethiae and geotrichum candidum co-culture / kontrola toksina t-2 u kokulturi fusarium langsethiae i geotrichum candidum. Archives of Industrial Hygiene and Toxicology **63**(4), 447–456 (2012). https://doi.org/10.2478/10004-1254-63-2012-2206
6. Gonzalez, R.C., Woods, R.E.: Digital Image Processing. Pearson (2018)
7. Hou, X., Chen, Y., Li, C., Wang, Y., Ma, X.: Use of the preservatives to control microbial contamination in plant tissue culture. Chinese Journal of Applied and Environmental Biology **29**(3), 730–735 (2023). https://doi.org/10.19675/j.cnki.1006-687x.2022.03052
8. Huang, J., Ahmed, T.S., Baranski, M., Lee, E., Chelvam, S.P., Wu, Y.Y., Ram, R., Rice, S., Yong, D., Springs, S.: Machine learning-aided at-line detection of bacterial marker na for cell manufacturing. In: Optics InfoBase Conference Papers (2021)
9. Isac, V., Cristea, C.: Rezults of microbial contamination in tissue culture laboratory of rifg pitesti. Scientific Papers of the Research Institute for Fruit Growing **27**(3) (2011)

ICCS Camera Ready Version 2026
To cite this paper please use the final published version:
DOI: 10.1007/978-3-032-29909-3_14

10. Kanavati, F., Tsuneki, M.: Partial transfusion: on the expressive influence of trainable batch norm parameters for transfer learning. In: Proceedings of Machine Learning Research, vol. 143, pp. 338–353 (2021)
11. Koptina, A., Strese, A., Backlund, A., Alsmark, C.: Challenges to get axenic cultures of trichomonas spp. — a new approach in eradication of contaminants and maintenance of laboratory microbiological cultures. Journal of Microbiological Methods **118**, 25–30 (2015). https://doi.org/10.1016/j.mimet.2015.08.009
12. Laitila, A., Sarlin, T., Kotaviita, E., Huttunen, T., Home, S., Wilhelmson, A.: Yeasts isolated from industrial maltings can suppress fusarium growth and formation of gushing factors. Journal of Industrial Microbiology & Biotechnology **34**(11), 701–713 (2007). https://doi.org/10.1007/s10295-007-0241-5
13. Launay, A., Perrin, G., Hirsch, E.: Vision based evaluation of the contamination level in high resolution images for industrial and clinical quality control applications. In: Fourteenth International Conference on Quality Control by Artificial Vision. vol. 86, p. 36. SPIE (2019). https://doi.org/10.1117/12.2521442
14. M.A. Saada, A., Al-Nur, E.A.: In vitro studies on the toxicity of culture filtrates of different fungi on the growth of fusarium oxysporum f.sp. vasinfectum. Journal of Biological Sciences **7**(2), 429–432 (2007). https://doi.org/10.3923/jbs.2007.429.432
15. Malik, P., Mukherjee, S., Mukherjee, T.K.: Microbial contamination of mammalian cell culture. In: Practical Approach to Mammalian Cell and Organ Culture, pp. 187–231. Springer Nature Singapore (2023). https://doi.org/10.1007/978-981-19-1731-8_5-1
16. Pandey, A., Sobita Simon, L., Ahmad, S.: Screening of antifungal activities in trichoderma isolates against some soil borne plant pathogens. National Academy Science Letters **33**(9-10), 285–288 (2010)
17. Qin, Q.M., Vallad, G.E., Subbarao, K.V.: Characterization of *Verticillium dahliae* and *V. tricorpus* isolates from lettuce and artichoke. Plant Disease **92**(1), 69–77 (2008). https://doi.org/10.1094/pdis-92-1-0069
18. Selvaraju, R.R., Cogswell, M., Das, A., Vedantam, R., Parikh, D., Batra, D.: Grad-cam: Visual explanations from deep networks via gradient-based localization. International Journal of Computer Vision **128**(2), 336–359 (2020). https://doi.org/10.1007/s11263-019-01228-7
19. Xia, M., Bao, P., Liu, A., Wang, M., Shen, L., Yu, R., Liu, Y., Chen, M., Li, J., Wu, X., Qiu, G., Zeng, W.: Bioleaching of low-grade waste printed circuit boards by mixed fungal culture and its community structure analysis. Resources, Conservation and Recycling **136**, 267–275 (2018). https://doi.org/10.1016/j.resconrec.2018.05.001
20. Zhang, Z.H., Yang, Z., Sun, Y., Wu, Y.F., Xing, Y.D.: Lenet-5 convolution neural network with mish activation function and fixed memory step gradient descent method. In: 2019 16th International Computer Conference on Wavelet Active Media Technology and Information Processing. IEEE (2019). https://doi.org/10.1109/iccwamtip47768.2019.9067661

ICCS Camera Ready Version 2026
To cite this paper please use the final published version:
DOI: 10.1007/978-3-032-29909-3_14